International Journal of General Medicine

Dovepress
Taylor & Francis Group

Open Access Full Text Article

ORIGINAL RESEARCH

Non-Invasive Diagnosis and Monitoring of Diabetic Nephropathy: Assessment of Renal Function and Fibrosis by Diffusion Kurtosis Imaging

Jian-Lei Yuan[1,2,*], Li-Ao Hu[1,2,*], Xin-Yu Wang[2,3,*], Zhao-Yu Shi[1,2], Ting Chen[1,2], Xin-Zhong Huang[1,2], Yu Wu[1,2], Qiu-Jie Cai[1,2], Zi-Xu Yang[1,2], Xin-Yi Chen[4], Li Yuan[1,2], Yuan Zhang[1,2]

[1]Department of Nephrology, Affiliated Hospital of Nantong University, Nantong, 226001, People's Republic of China; [2]Medical School of Nantong University, Nantong, 226001, People's Republic of China; [3]Department of Medical Imaging, Affiliated Hospital of Nantong University, Nantong, 226001, People's Republic of China; [4]Nanjing Medical University School of Basic Medical Sciences, Nanjing, 211166, People's Republic of China

*These authors contributed equally to this work

Correspondence: Yuan Zhang; Li Yuan, Email zhangy.nt.nd@ntu.edu.cn; yuanlint@163.com

Background: This monocentric, cross-sectional study explored the use of diffusion kurtosis imaging (DKI) as a non-invasive means to diagnose and monitor diabetic nephropathy (DN).

Methods: Patients with diabetes mellitus (DM, n = 11), mild DN (N = 14), and severe DN (n = 29) were recruited. Eight DKI metrics (MK, MD, Da, Dr, Ka, Kr, FA, FAk) were determined from the imaging results, and their correlations with routine laboratory results were analyzed. The receiver operating characteristic (ROC) curves were plotted, and the diagnostic value of the DKI metrics was analyzed. In addition, renal biopsy was carried out for ten DN patients who had appropriate indications. Their interstitial fibrosis and tubular atrophy (IFTA) score and the fibrosis ratio of cortical area (F%) were analyzed in combination with the DKI metrics.

Results: The progression of DN, reflected by the estimated glomerular filtration rate (eGFR), was accompanied by rising mean kurtosis (MK) and axial kurtosis (Ka) along with decreasing mean diffusivity (MD), axial diffusivity (Da), and radial diffusivity (Dr). Whereas MK was correlated negatively with hemoglobin (Hb) and eGFR and positively with neutrophil gelatinase-associated lipocalin (NGAL), cystatin C (CysC), and serum creatinine (Scr), MD, Da, and Dr were positively correlated with Hb and eGFR and negatively correlated with CysC and Scr. For the biopsied patients, MK was positively correlated with IFTA, and fractional anisotropy of kurtosis (FAk) was negatively correlated with F% and IFTA. Among the DKI indicators, MK had the highest AUC (0.922, 95% CI: 0.843–1.000).

Conclusion: The noninvasive monitoring of DN was feasible with DKI, and MK could indicate the renal function and fibrosis of DN patients. Changes in MK may also serve as a biomarker to assess treatment response (eg, microstructural improvement) after therapeutic interventions (eg, drug therapy for diabetic nephropathy, anti-fibrotic therapy).

Plain Language Summary: Diabetic nephropathy (DN) is a serious kidney complication of diabetes and the leading cause of end-stage renal disease. While imaging tools like ultrasound, CT, and standard MRI are widely used to evaluate kidney structure and blood flow, they play a limited role in diagnosing or monitoring DN. There is a growing need for non-invasive methods that can detect early changes and track disease progression more precisely. Diffusional Kurtosis Imaging (DKI) is an advanced MRI technique that captures the complexity of water movement in tissues, offering insights into kidney microstructure. The present study analyzed, in DN patients, eight DKI metrics—mean kurtosis and diffusivity (MK and MD), axial and radial diffusivity and kurtosis (Da, Dr, Ka, Kr,), fractional anisotropy (FA), and fractional anisotropy in kurtosis (FAk)—and compared them to standard lab markers and biopsy results. Among all DKI measures, MK showed the strongest correlation with kidney function and fibrosis. Specifically, higher MK values were associated with worse kidney function (lower hemoglobin and eGFR, higher creatinine, NGAL, and cystatin C) and more severe tissue damage (higher fibrosis scores on biopsy). MK also achieved the highest diagnostic accuracy (AUC = 0.922) in distinguishing disease

Received: 15 January 2025
Accepted: 18 July 2025
Published: 21 July 2025

severity. These findings suggest that DKI, and MK in particular, can serve as a powerful, non-invasive biomarker for assessing kidney damage and fibrosis in DN patients. MK may also help track treatment response, offering a way to monitor improvements in kidney microstructure following therapies.

Keywords: diabetes mellitus, diabetic nephropathy, diffusion kurtosis imaging, magnetic resonance imaging, mean kurtosis

Introduction

Diabetic nephropathy (DN) is a serious complication of diabetes that affects the kidneys and is the leading cause of end-stage renal disease (ESRD).[1] For DN patients, chronic hyperglycemia damages their glomeruli, thus reducing their kidney function, and the damage is exacerbated by hypertension and other metabolic disturbances.[2] The early stages of DN often have no symptoms, and upon disease progression, symptoms include proteinuria, edema, hypertension, etc.[3] Current clinical guidelines emphasize a comprehensive approach to manage DN and prevent ESRD, including lifestyle changes, controlling blood glucose and blood pressure, and using appropriate medications to reduce proteinuria and slow disease progression.[3]

The progression of DN is difficult to detect and quantify, and there is a strong clinical demand for the rapid, accurate, and non-invasive diagnosis and monitoring of DN. The diagnosis of DN typically involves urine tests to detect proteinuria, blood tests to assess kidney function (eg, serum creatinine, glomerular filtration rate), and at times even kidney biopsies.[4] The amount of advanced glycation end products in the lens has been measured by scan fluorescence to infer the cumulative blood glucose exposure and kidney damage.[5] Specialized electronic nose systems have been developed to detect volatile organic compounds associated with kidney diseases in the patient's breath.[6] However, well-established radiology methods, including Doppler ultrasound, magnetic resonance imaging (MRI), computed tomography (CT), while powerful in assessing the kidney size, blood flow, structural abnormalities, etc, have remained relatively secondary in the diagnosis and monitoring of DN.

Diffusional Kurtosis Imaging (DKI) is an advanced MRI technique that extends the capabilities of traditional diffusion-weighted imaging (DWI) and diffusion tensor imaging (DTI).[7,8] It measures the non-Gaussian diffusion of water molecules in biological tissues and accounts for the deviations of water diffusion from Gaussian distribution, thus providing a more accurate representation of tissue microstructure.[9] It is particularly useful in the diagnosis of brain tumors, neurodegenerative diseases, traumatic brain injury, stroke, psychiatric disorders, etc.[10–15] It has been used to assess renal function and fibrosis,[6,16–18] and ongoing research is expanding its clinical applications to oncology and other areas.[19–21]

Some research has shown that DKI findings may correlate well with various conventional laboratory biomarkers. For instance, DKI-derived parameters such as mean kurtosis (MK) and apparent diffusion coefficient (ADC) have been correlated with estimated glomerular filtration rate (eGFR), a key blood biomarker for kidney function, and lower MK and ADC values were associated with worse renal function.[18,22] It has also been reported that DKI can effectively differentiate severe and mild renal fibrosis, which is often assessed through urine tests for proteinuria and other markers.[22] These findings highlight the potential of DKI as a valuable tool in medical imaging, providing insights that align with conventional laboratory tests and offering a non-invasive means to monitor and predict disease outcomes. Hence, this study aimed to find out among all DKI parameters, which can be used to assess renal function and detect renal tissue fibrosis, to thus develop a non-invasive means to diagnose and monitor diabetic nephropathy.

Materials and Methods

Patients

Patients admitted to Affiliated Hospital of Nantong University from September 2020 through September 2023 were approached, including DN patients from the Nephrology Department and patients from the Endocrinology Department diagnosed with diabetes mellitus (DM). All diagnoses were based on the guidelines of the American Diabetes Association and the American Kidney Fund. Diabetic nephropathy was confirmed when DM was identified as the

cause of renal damage, other causes of chronic kidney disease (CKD) were excluded, and at least one of the following applied: (1) urinary albumin creatinine ratio (uACR) above 30 mg/g, (2) estimated glomerular filtration rate (eGFR) remaining below 60 mL/min/1.73 m^2 for three or more consecutive months, or (3) steady decline of eGFR despite normal uACR (<30 mg/g). Patients were excluded from the DN cohort if they met any of the exclusion criteria:

1. Type 1 diabetes (T1DM) with a short course (<5 years) or no diabetic retinopathy,
2. Decline of eGFR by more than 30 mL/min/1.73 m^2 in the past month,
3. Increase of urine protein by 0.3 g/24 h in the past month,
4. Resistant hypertension,
5. Appearance of active urinary sediment (red blood cells, white blood cells, etc),
6. Symptoms or signs of other systemic diseases,
7. Decrease of eGFR by more than 30% in 2 to 3 months after the administration of angiotensin converting enzyme inhibitor (ACEI) or angiotensin receptor blocker (ARB), or
8. Abnormal renal ultrasound findings.

The DN patients were divided into two groups based on their eGFR: Group Mild, >60 mL/min/1.73 m^2; Group Severe, ≤60 mL/min/1.73 m^2. The DM patients formed the control group denoted as Group DM.[23]

This research project was approved by the Ethical Committee of Affiliated Hospital of Nantong University (approval No. 2019-K070) and complied with the principles of the Declaration of Helsinki. Written informed consent was obtained from all participants.

Clinical and Biochemical Parameters

The following clinical parameters were measured: from the venous blood sample, hemoglobin (Hb), hematocrit (HCT), serum creatinine (Scr), albumin (ALB), cystatin C (CysC), and neutrophil gelatinase-associated lipocalin (NGAL); from the 24-hour urine specimen, uACR and 24-hour urine protein. The calculation of eGFR used the Chronic Kidney Disease Epidemiology Collaboration (CKD-EPI) equations given by Levey et al:[24]

$$\mathrm{eGFR} = 141 \times \min(\mathrm{Scr}/\kappa, 1)^{\alpha} \times \max(\mathrm{Scr}/\kappa, 1)^{-1.209} \times 0.993^{\mathrm{age}} \ (\times 1.018 \ [\text{if female}])$$

where eGFR is the estimated glomerular filtration rate (mL/min/1.73 m^2), Scr is the serum creatinine (mg/dL), age is expressed in years, κ takes 0.7 for females and 0.9 for males, and α takes −0.329 for females and −0.411 for males, respectively.

Renal Pathological Analysis

Ultrasound-guided renal biopsy was carried out for DN patients who had indications for renal biopsy and agreed to the operation. The renal biopsy operation was performed after completing the MRI examination. Before the operation, the risks and precautions were explained to the patients, who then signed the consent form before proceeding. The collected samples were fixed with formaldehyde and sliced into 2 μm thin sections. The frozen tissues were examined by immunofluorescence (IgG, IgA, IgM, C3, C1q, fibrin-related antigen), light microscopy (after H&E, PAS, PASM, and Masson trichrome staining), and electron microscopy. The interstitial fibrosis and tubular atrophy (IFTA) score[25] and the fibrosis ratio of cortical area (F%) were determined for all patients.

MRI Protocol

Diffusion kurtosis imaging of both kidneys was performed on a GE Discovery 3T MR750w scanner using a 16-channel phased-array abdomen coil. The b-value was 0, 400, 800, 1200, 1600, and 2000s/mm^2. Other parameters were as follows: repetition time, 3158 ms; echo time, 92.2 ms; layer thickness, 5 mm; matrix size, 128 mm × 128 mm; number of sections, 8; layer interval, 0; field of view (FOV) dimension, 320 mm × 320 mm; acceleration factor, 2; excitation number, 2; flip angle, 90°. All patients fasted for 6–8 h (no food or water) before the exam.

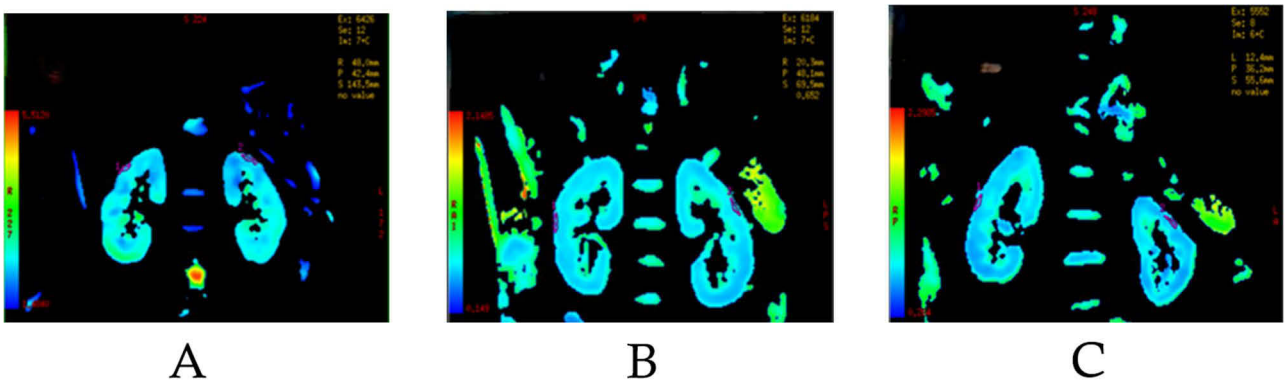

Figure 1 Representative renal MRI images. (**A**) Patient diagnosed with diabetes (Group DM). (**B**) Patient diagnosed with diabetic nephropathy and eGFR > 60 mL/min/1.73 m^2 (Group Mild). (**C**) Patient diagnosed with diabetic nephropathy and eGFR ≤ 60 mL/min/1.73 m^2 (Group Severe).

Image Analysis

The uploaded DKI data were analyzed using GE Advantage Workstation 4.6. The DKI parameters were generated by the post-processing software programs. For both kidneys, the regions of interest (ROIs) in the renal cortices were drawn manually by two certified radiologists. Figure 1 shows the example DKI images. The radiologists and the data analysts were all blinded. The following values were measured from the DKI maps: mean kurtosis (MK), mean diffusivity (MD), axial diffusivity (Da), radial diffusivity (Dr), axial kurtosis (Ka), radial kurtosis (Kr), fractional anisotropy (FA), and fractional anisotropy of kurtosis (FAk). In all cases the average value of two measurements was taken.

Sample Size

A pre-hoc power analysis (G*Power 3.1.9.7) was conducted during the study design phase. Based on prior MRI studies of early DN, we anticipated a standardized effect size (Cohen's d) of ≥0.6 between healthy controls and early DN groups. For a two-sided independent *t*-test (α = 0.05, power = 80%), this yielded a requirement of 45 subjects per group. Accounting for a 10% attrition rate, we initially targeted 50 participants per group.

Statistical Analysis

All data were analyzed using SPSS 25.0 for Windows (IBM Corp., Armonk, NY USA). The normality of data was verified by the Shapiro–Wilk test. Normally distributed variables were expressed mean ± standard deviation and the differences between groups were identified by one-way analysis of variance (ANOVA) and post-hoc comparisons (Bonferroni correction). Data with a skewed distribution were expressed by their mean and the interquartile range (P25, P75) and compared pairwise by the Kruskal–Wallis test. Categorical variables were expressed as numbers (n) and percentages (%). Inter-rater reliability was characterized by the intraclass correlation (ICC), and the reliability was deemed high when the ICC value was over 0.8. The Pearson's correlation coefficients (r) between the clinical parameters of DN patients and the DKI metrics were calculated. The diagnostic performance of the DKI metrics was assessed by drawing the receiver-operating characteristic (ROC) curves and measuring the corresponding area under the curves (AUCs). In all cases, differences between groups were considered statistically significant when $P < 0.05$ (two-tailed).

Results

Characteristics and Clinical Parameters

Fifty-four patients were enrolled in this study (Table 1). Group DM had 11 patients, including 3 males and 8 females, with an average age of 61.00 ± 6.90 years. Group Mild had 14 patients, including 11 males and 3 females, with an average age of 53.50 ± 9.38 years. Group Severe had 29 patients, including 19 males and 10 females, with an average age of 54.90 ± 11.92 years.

Table 1 Patient Information

Characteristic	DM patients	DN patients		P_0§	P_1§	P_2§	P_3§
	Group DM N = 11	Group Mild N = 14	Group Severe N = 29				
Age (years)	61.00 ± 6.90	53.50 ± 9.38	54.90 ± 11.92	0.176	0.188	0.237	0.912
Sex (M/F)	3/8	11/3[a]	19/10	0.027	0.029	0.085	>0.999
BMI (kg/m^2)	25.00 [22.20, 27.50]	25.26 [22.43, 28.20]	25.60 [23.16, 27.39]	0.754	>0.999	>0.999	>0.999
Systolic BP (mmHg)	133.82 ± 18.21	143.14 ± 21.57	149.83 ± 17.95	0.075	0.275	0.082	>0.999
Diastolic BP (mmHg)	76.09 ± 10.75	77.79 ± 9.48	82.03 ± 8.06	0.124	>0.999	0.206	0.382
Urine protein (g/24h)	1.38 [0.10, 3.04]	2.58 [1.69, 4.40]	3.97 [1.31, 7.82]	0.091	0.704	0.122	0.711
Hb (g/L)	135.00 ± 11.96	121.64 ± 16.49	100.07 ± 19.61[ab]	<0.001	0.153	<0.001	0.001
HCT (%)	0.40 ± 0.03	0.36 ± 0.05	0.30 ± 0.05[ab]	<0.001	0.186	<0.001	0.002
NGAL	104.25 ± 9.05	262.18 ± 147.86	344.57 ± 107.33 [a]	0.037	0.308	0.031	0.435
ALB (g/L)	38.70 ± 6.81	27.74 ± 7.39[a]	32.19 ± 7.01 [a]	0.002	0.002	0.052	0.301
uACR (mg/g)	3.62 [1.51, 26.28]	139.06 [69.97, 482.34][a]	205.87 [52.08, 510.53][a]	0.001	0.006	0.001	>0.999
CysC (mg/L)	0.64 [0.59, 0.75]	0.87 [0.73, 1.14]	2.43 [1.86, 2.77][ab]	<0.001	0.532	<0.001	<0.001
Scr (μmol/L)	48.00 [46.00, 58.00]	84.00 [62.00, 102.00]	267.00 [194.00, 336.00] [ab]	<0.001	0.300	<0.001	<0.001
eGFR (mL/min/1.73m^2)	106.09 [100.56, 114.50]	91.27 [70.08, 112.58]	17.68 [13.98, 33.92][ab]	<0.001	>0.999	<0.001	<0.001

Notes: [a] $P < 0.05$ vs Group DM. [b] $P < 0.05$ vs Group Mild. § P_0, multigroup comparison; P_1, Group DM vs Group Mild; P_2, Group DM vs Group Severe; P_3, Group mild vs Group Severe. *P* values are typeset in boldface if they are less than 0.05.

Abbreviations: DM, diabetes mellitus; DN, diabetic nephropathy; BMI, body mass index; BP, blood pressure; Hb, hemoglobin; HCT, hematocrit; NGAL, neutrophil gelatinase-associated lipocalin; ALB, albumin; uACR, urinary albumin creatinine ratio; CysC, cystatin C; SCr, serum creatinine; eGFR, estimated glomerular filtration rate.

Among the three groups, no significant differences in age, body mass index, blood pressure (both systolic and diastolic), 24-hour urine protein, and uACR ($P > 0.05$). Compared to Group DM and Group Mild, Group Severe had higher CysC and Scr, but lower Hb, HCT and eGFR. Group Severe also had significantly higher NGAL than Group DM. Both Group Mild and Group Severe had significantly lower ALB ($P < 0.05$). The progression of DN was accompanied by the escalation of NGAL, CysC, Scr and the decline of HCT, ALB, and eGFR ($P < 0.05$).

Renal DKI Metrics

Figure 2 and Table 2 summarize the DKI metrics of the three groups. Compared to Group DM and Group Mild, Group Severe had higher MK and Ka values and lower MD and Dr values ($P < 0.05$). However, these metrics did not differ significantly between Group DM and Group Mild ($P > 0.05$). Group Severe also had higher Da value than Group DM ($P < 0.05$) but not than Group Mild. For all three groups, no significant difference existed in Kr, FA, and FAk. For all three groups, no significant difference existed in Kr, FA, and FAk.

Reliability

Table 3 shows that for all DKI metrics, the ICCs values ranged between 0.867 and 0.943, which indicated excellent consistency between the results given by the two raters. Hence, for the subsequent analyses, the result from a single rater was selected randomly and used.

Correlation Between DKI Metrics and Laboratory Assay Results

Both Hb and eGFR were negatively correlated with MK and positively correlated with MD, Da, and Dr. Both CysC and Scr were correlated positively with MK and negatively correlated with MD, Da, and Dr. In addition, MK was correlated positively with NGAL (Table 4, Figures 3–6).

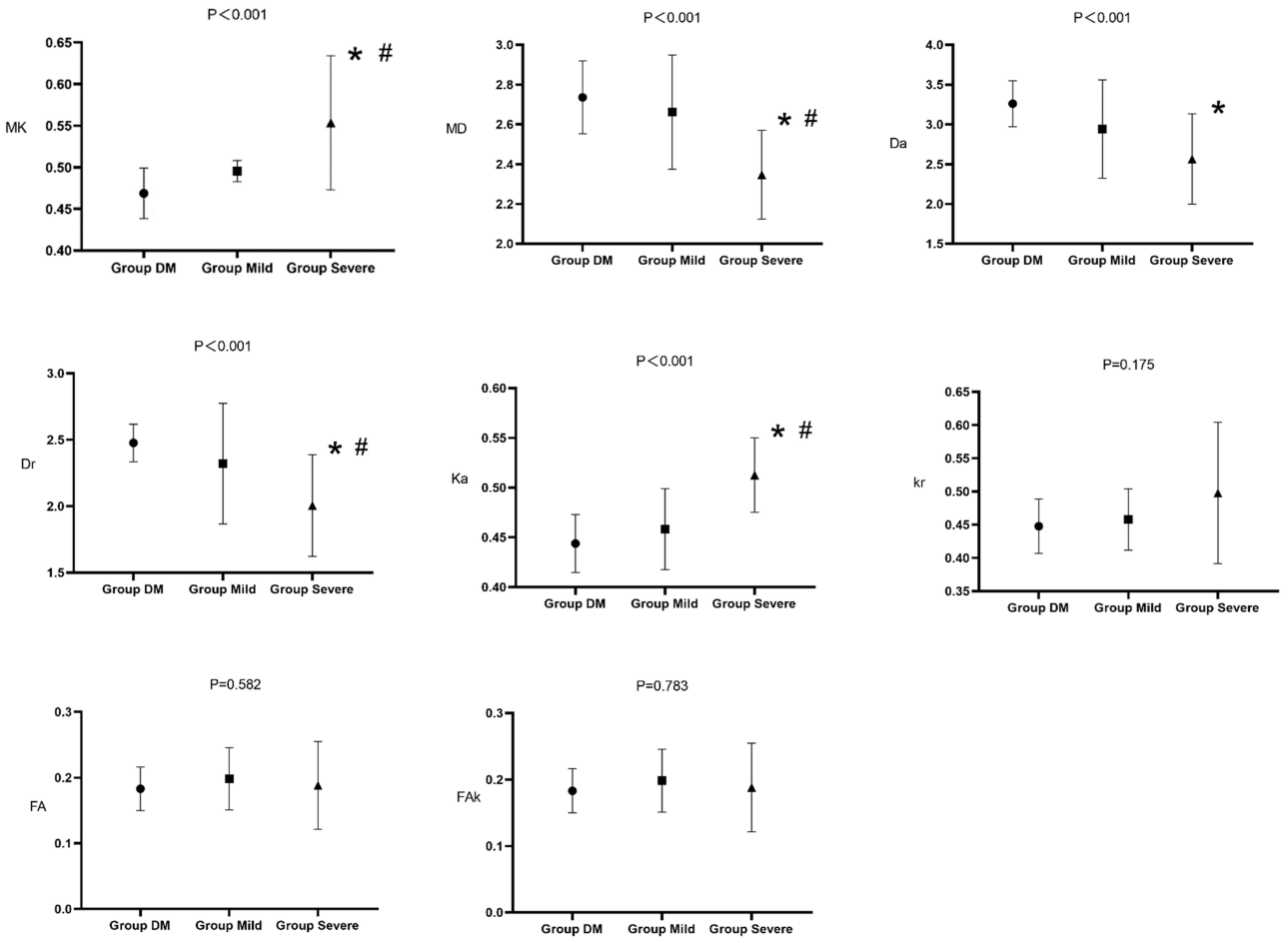

Figure 2 Comparisons of DKI metrics between groups. Group DM, patients diagnosed with diabetes; Group Mild, patients diagnosed with diabetic nephropathy with eGFR > 60 mL/min/1.73 m^2; Group Severe, patients diagnosed with diabetic nephropathy and eGFR ≤ 60 mL/min/1.73 m^2. * $P < 0.05$ vs Group DM. # $P < 0.05$ vs Group Mild.

Abbreviations: MK, mean kurtosis; MD, mean diffusivity; Da, axial diffusivity; Dr, radial diffusivity; Ka, axial kurtosis; Kr, radial kurtosis; FA, fractional anisotropy; FAk, fractional anisotropy of kurtosis.

Correlation Between DKI Metrics and Pathological Parameters of Renal Biopsy

The ten patients receiving renal biopsy distributed as follows (Table 5, Figure 7). Among these patients, a positive correlation existed between MK and IFTA, whereas FAk was negatively correlated with IFTA and F% (Table 6).

Table 2 Summary of Imaging Data

Metrics	DM patients	DN patients		*P0*§	P_1§	P_2§	P_3§
	Group DM	Group Mild	Group Severe				
	N = 11	N = 14	N = 29				
MK	0.47 [0.44, 0.49]	0.49 [0.48, 0.50]	0.52 [0.51, 0.57] [ab]	<0.001	0.845	<0.001	0.005
MD	2.74 ± 0.18	2.66 ± 0.29	2.35 ± 0.22[ab]	<0.001	0.712	<0.001	0.001
Da	3.26 ± 0.29	2.94 ± 0.62	2.56 ± 0.57 [a]	<0.001	0.413	0.001	0.080
Dr	2.48 ± 0.14	2.32 ± 0.45	2.01 ± 0.38 [ab]	0.001	0.552	0.002	0.030

(*Continued*)

Table 2 (Continued).

Metrics	DM patients	DN patients		*P0*§	P_1§	P_2§	P_3§
	Group DM	Group Mild	Group Severe				
	N = 11	N = 14	N = 29				
Ka	0.44 ± 0.03	0.46 ± 0.04	0.51 ± 0.04 [ab]	<0.001	0.598	<0.001	<0.001
Kr	0.45 ± 0.04	0.46 ± 0.05	0.50 ± 0.11	0.175	>0.999	0.269	0.707
FA	0.18 ± 0.03	0.20 ± 0.05	0.19 ± 0.07	0.582	>0.999	>0.999	0.930
FAk	0.17 ± 0.08	0.23 ± 0.10	0.22 ± 0.12	0.373	0.387	0.440	0.951

Notes: [a] $P < 0.05$ vs Group DM. [b] $P < 0.05$ vs Group mild. § P_0, multigroup comparison; P_1, Group DM vs Group Mild; P_2, Group DM vs Group Severe; P_3, Group mild vs Group Severe. *P* values are typeset in boldface if they are less than 0.05.
Abbreviations: DM, diabetes mellitus; DN, diabetic nephropathy; MK, mean kurtosis; MD, mean diffusivity; Da, axial diffusivity; Dr, radial diffusivity; Ka, axial kurtosis; Kr, radial kurtosis; FA, fractional anisotropy; FAk, fractional anisotropy of kurtosis.

Table 3 Inter-Rater reliability of Renal DKI Metrics

DKI metrics (cortex)	ICC	95% CI
MK	0.943	0.925–0.967
MD	0.912	0.893–0.935
Da	0.935	0.918–0.951
Dr	0.898	0.865–0.914
Ka	0.902	0.884–0.923
Kr	0.887	0.862–0.891
FA	0.867	0.844–0.885
FAk	0.921	0.903–0.938

Abbreviations: DKI metrics (cortex), Metrics of diffusion kurtosis imaging of renal cortex; ICC, intraclass correlation; CI, confidence interval; MK, mean kurtosis; MD, mean diffusivity; Da, axial diffusivity; Dr, radial diffusivity; Ka, axial kurtosis; Kr, radial kurtosis; FA, fractional anisotropy; FAk, fractional anisotropy of kurtosis.

Table 4 Correlation Between Renal DKI Metrics and Clinical Parameters of All DN Patients

	MK		MD		Da		Dr	
	r	*P*	*r*	*P*	*r*	*P*	*r*	*P*
Urine protein (g/24 h)	0.313	0.071	−0.220	0.161	−0.308	0.047	−0.189	0.230
Hb (g/L)†	−0.527	**<0.001**	0.488	**<0.001**	0.507	**<0.001**	0.498	**<0.001**
NGAL†	0.531	**0.028**	−0.338	0.115	−0.327	0.128	−0.329	0.125
ALB (g/L)†	−0.270	0.088	0.030	0.829	0.165	0.236	0.178	0.203
CysC (mg/L)†	0.745	**<0.001**	−0.606	**<0.001**	−0.488	**<0.001**	−0.602	**<0.001**
SCr (μmol/L)†	0.748	**<0.001**	−0.612	**<0.001**	−0.521	**<0.001**	−0.643	**<0.001**
eGFR (mL/min/1.73 m^2)†	−0.751	**<0.001**	0.632	**0.001**	0.502	**<0.001**	0.612	**<0.001**

Note: *P* values are typeset in boldface if they are less than 0.05.
Abbreviations: MK, mean kurtosis; MD, mean diffusivity; Da, axial diffusivity; Dr, radial diffusivity; Hb, hemoglobin; NGAL, neutrophil gelatinase-associated lipocalin; ALB, albumin; CysC, cystatin C; SCr, serum creatinine; eGFR, estimated glomerular filtration rate.

Diagnostic Value of DKI Metrics

Table 7 summarizes the parameters of the ROC curves of different DKI metrics (Figure 8). The ROC curves were created based on how well the metrics distinguished Group Severe from the other two groups, since significant differences were

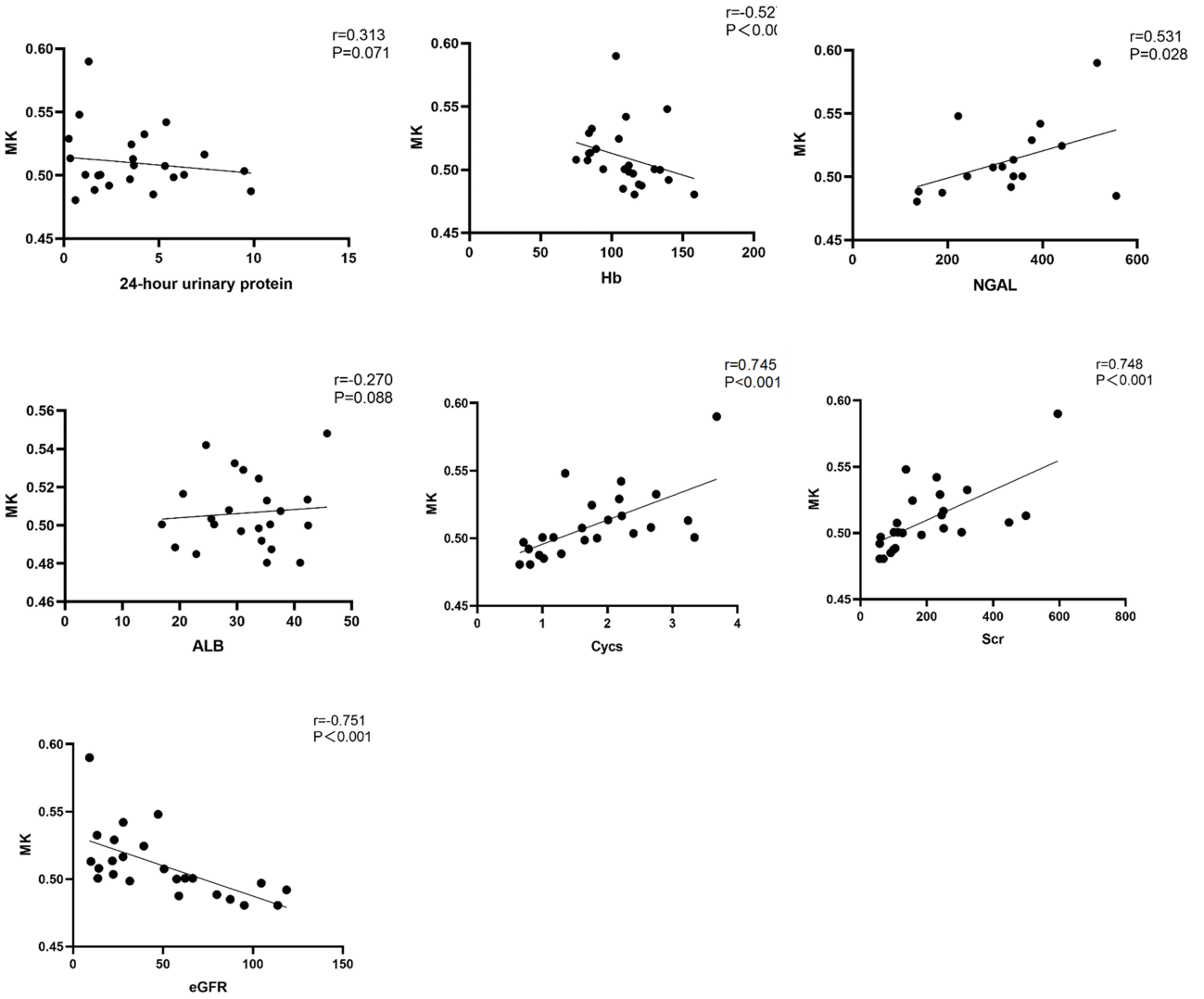

Figure 3 Correlation between MK and laboratory test results.
Abbreviations: MK, mean kurtosis; Hb, hemoglobin; NGAL, neutrophil gelatinase-associated lipocalin; ALB, albumin; CysC, cystatin C; SCr, serum creatinine; eGFR, estimated glomerular filtration rate.

frequently lacking between Group Severe and Group Mild. The ROC curves could not be plotted for Kr, FA, and FAk due to the lack of statistical significance. Gratifyingly, superior diagnostic value was found for MK. With the optimal cut-off value at 0.49, the sensitivity was 83.3% and the specificity was 94.4% ($P < 0.001$).

Discussion

Due to inherent clinical constraints, including stringent biopsy indications (eg, proteinuria thresholds, renal function criteria, and patient consent), the recruitment of biopsy-confirmed DN cases proved challenging. The final cohort comprised 54 patients: 11 controls, 14 mild DN, and 29 severe DN cases. While this patient pool fell below the ideal size, it reflected consecutive enrollment (all eligible biopsy patients were from a single center over 5 years), rigorous matching, and strict adherence to KDIGO diagnostic criteria. Despite the reduced power, several parameters achieved statistical significance ($P < 0.05$), suggesting clinically meaningful effects. Non-significant trends in other metrics may reflect type II error due to sample limitations—a common challenge in imaging studies of biopsy-stratified cohorts. This work provides essential preliminary data for future large-scale validation.

Gaussian water diffusion, which assumes that water molecules move randomly in a uniform and unrestricted manner following a normal distribution (bell curve), is the basis for DWI and DTI, which measures the overall diffusion of water

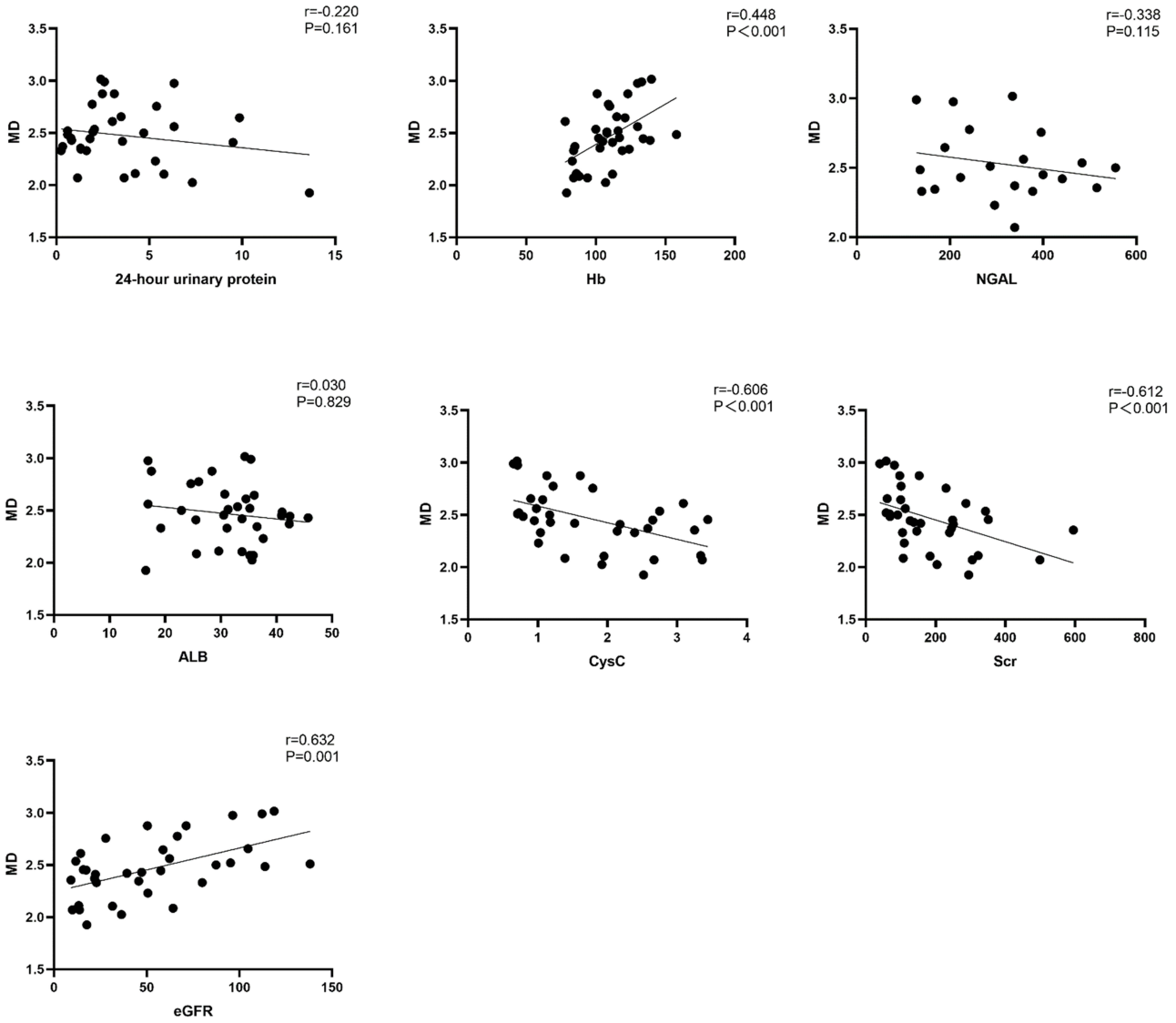

Figure 4 Correlation between MD and laboratory test results.
Abbreviations: MD, mean diffusivity; Hb, hemoglobin; NGAL, neutrophil gelatinase-associated lipocalin; ALB, albumin; CysC, cystatin C; SCr, serum creatinine; eGFR, estimated glomerular filtration rate.

molecules and the directionality of water diffusion within tissues, respectively. However, the diffusion of water in the kidney is not Gaussian, as the cell membranes, intracellular organelles, and various other renal structures restrict water diffusion.[18,26–30] In contrast, DKI can process non-Gaussian diffusion, and it can thus detect subtle changes in tissue microstructures that are not visible with DWI or DTI.[8] By capturing the complexity of water movement in the renal tissue, DKI can reflect the heterogeneity of the microenvironment.

Among the DKI metrics, MK could very well distinguish Group Severe from Group Mild and Group DM, and its AUC value (0.922) was the highest. It was correlated highly negatively with Hb and eGFR and highly positively with CysC and Scr. However, Group Mild and Group DM were indistinguishable by MK. It has been reported that the decline in eGFR is accompanied by rising MK,[18] and the correlation between MK and tissue integrity has been verified for brain,[31–33] liver,[34] prostate,[35] etc. In terms of damaging the renal structure, DN can cause glomerulosclerosis, chronic interstitial nephritis, arterionephrosclerosis, tubular lesions, papillary necrosis, etc. The rising MK value (Table 2) likely reflected the initial changes in these lesions. The IFTA score is an important predictor for the prognosis of DN patients,[36] and a significantly positive correlation existed between MK and IFTA (Table 6). Interestingly, MK had a significantly

https://doi.org/10.2147/IJGM.S517683

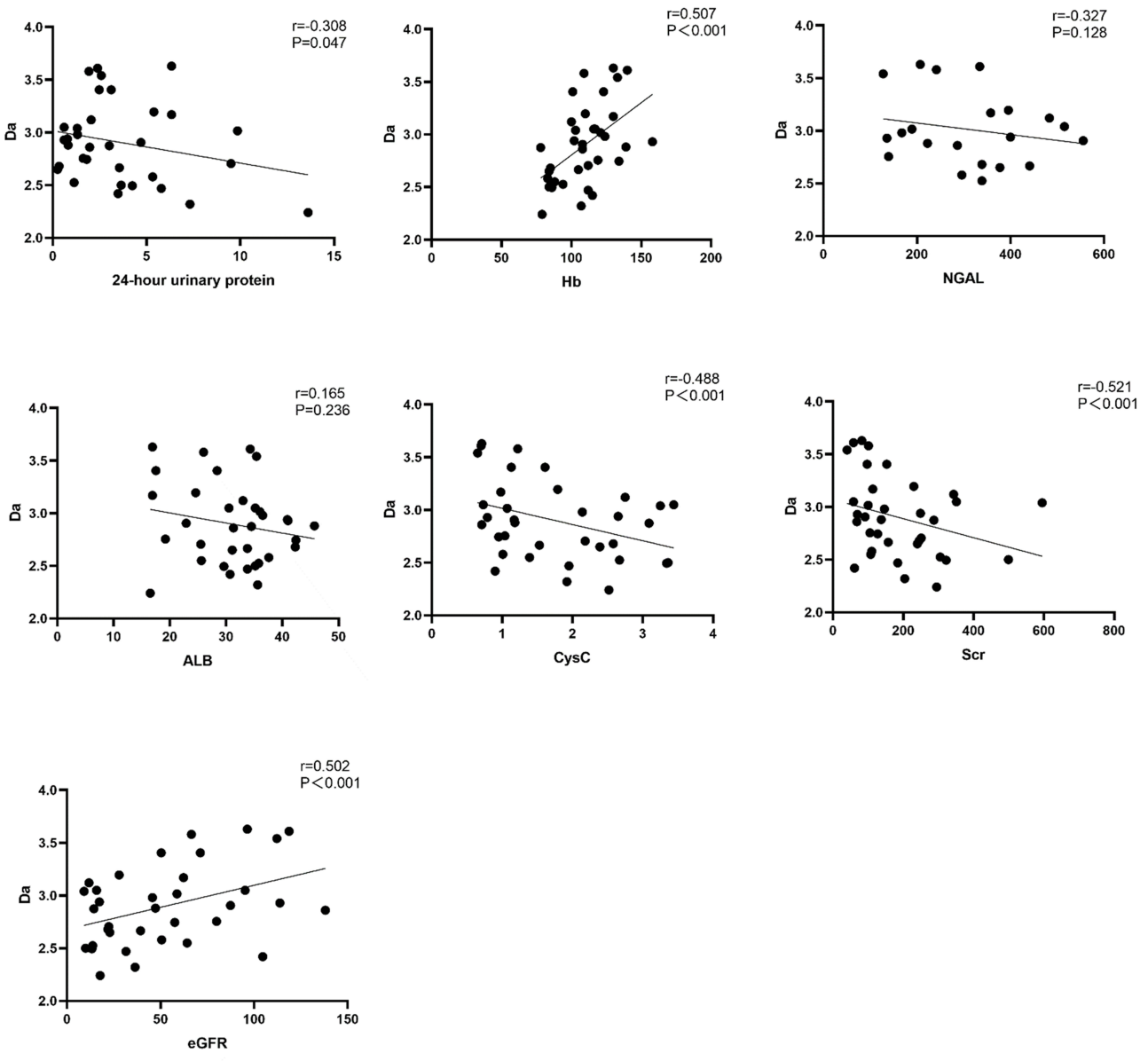

Figure 5 Correlation between Da and laboratory test results.
Abbreviations: Da, axial diffusivity; Hb, hemoglobin; NGAL, neutrophil gelatinase-associated lipocalin; ALB, albumin; CysC, cystatin C; SCr, serum creatinine; eGFR, estimated glomerular filtration rate.

negative correlation with Hb (Table 4). To the best of our knowledge, this is the first report of an association between Hb and MK in humans. Renal ischemia can cause several cellular changes, including cell membrane shrinkage,[37] cell matrix hyperplasia,[38] and endothelial cell death.[39] The decline in Hb was likely due to insufficient perfusion of the renal tissue, which is a significant factor in the development and progression of ESRD.[36] Deteriorating renal function reduces erythropoietin (EPO) production, which contributes to decreased hemoglobin levels and anemia. Presumably, the progression of kidney disease reduces renal microvessels and aggravates of fibrosis, which increases MK values. Hemoglobin and MK may be indirectly associated because they both reflect kidney disease severity. Renal anemia (decreased hemoglobin) usually occurs only in the later stages of renal disease. While Group Severe can be distinguished from the other two groups based on the MK value, Group Mild and Group DM were not distinguishable by their MK values ($P > 0.05$). That is, MK does not capture the early microvascular changes in the renal cortex of DN patients.

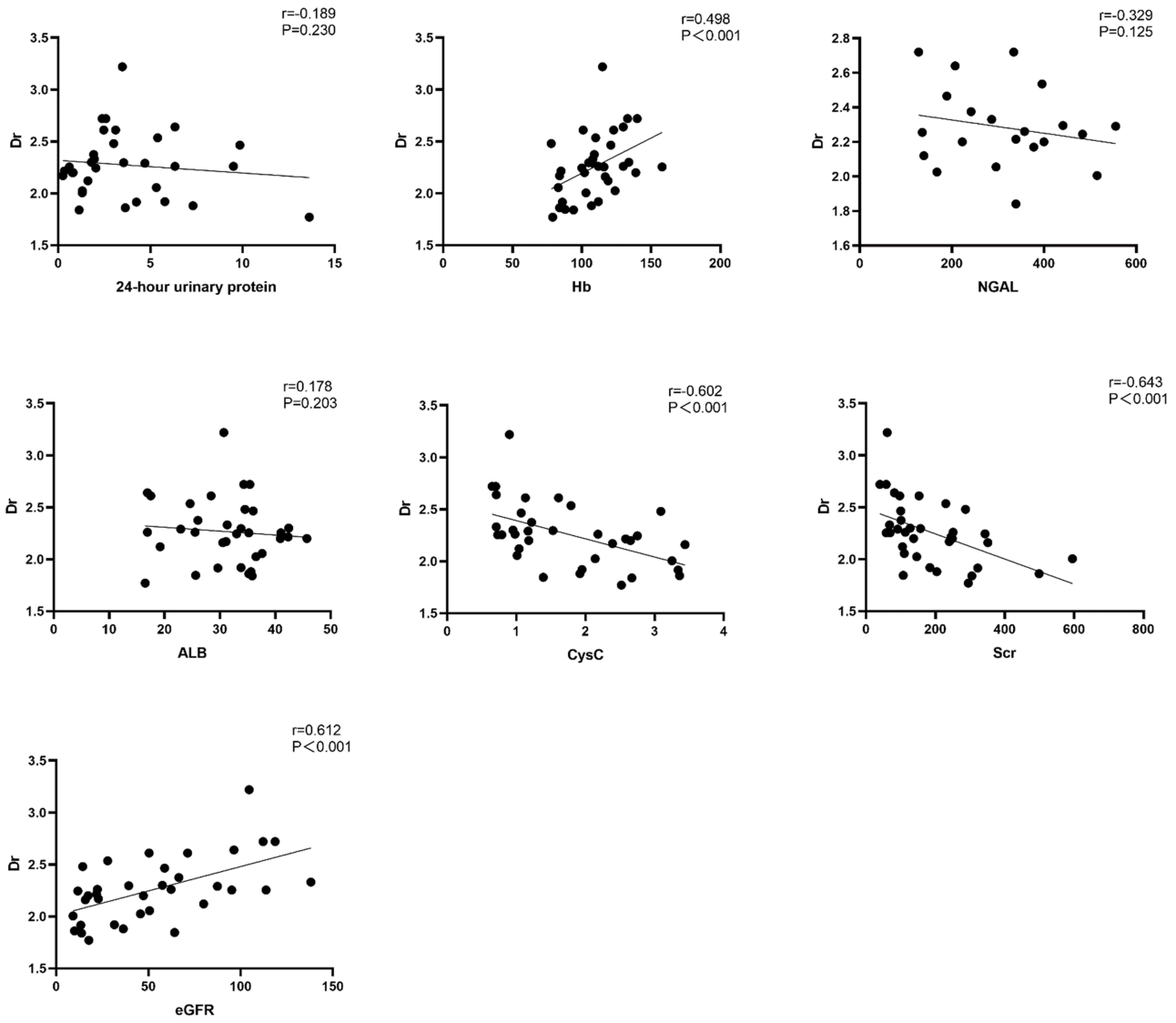

Figure 6 Correlation between Dr and laboratory test results.
Abbreviations: Da, radial diffusivity; Hb, hemoglobin; NGAL, neutrophil gelatinase-associated lipocalin; ALB, albumin; CysC, cystatin C; SCr, serum creatinine; eGFR, estimated glomerular filtration rate.

Intriguingly, it has been reported that the renal cortex of diabetic rats has elevated MK values, which may be relevant to the peculiarities of the kidney of rats.[18]

Previous research suggested that MD is a less sensitive biomarker for DN than MK. Presumably, the pathological changes associated with cellular damage restrict water diffusion and reduce MD.[40] In this work, although MD is also correlated with Hb and eGFR significantly negatively and with CysC and Scr significantly positively, it had an inferior diagnostic efficacy (AUC = 0.865) compared to MK. In addition, Unlike MK, MD was not correlated with IFTA statistically significantly. It has been reported that for IgA nephropathy patients, cortex MK can provide valuable information, but MD cannot.[41]

Previous studies on Da, Dr, and Ka have focused on the nervous system, tumors, etc, and their utility in evaluating kidney disease is poorly understood. This work for the first time explored their diagnostic value in DN. Table 4 shows that they correlated well with clinical indicators, and Table 7 shows that they had good diagnostic performance. In a study on primary aldosteronism (PA), researchers applied multiple DWI models to renal MRI to assess kidney diffusion parameters (medullary MD, Dr, and FA, cortical FA and Da) and noted significant differences between PA patients and

https://doi.org/10.2147/IJGM.S517683

Table 5 Summary of Renal Biopsy Results and DKI Data

Patient	F%	IFTA	MK	MD	Da	Dr	Ka	Kr	FA	FAk
1	5	1	0.497	2.655	2.420	3.220	0.426	0.450	0.250	0.303
2	0	1	0.508	2.230	2.580	2.055	0.538	0.455	0.168	0.273
3	15	1	0.501	2.560	3.170	2.260	0.464	0.449	0.230	0.256
4	8	1	0.465	2.875	3.405	2.610	0.411	0.413	0.187	0.283
5	8	1	0.489	2.330	2.755	2.120	0.522	0.446	0.188	0.277
6	10	1	0.428	2.990	3.540	2.720	0.417	0.390	0.180	0.233
7	15	1	0.439	2.345	2.980	2.025	0.466	0.432	0.266	0.419
8	40	2	0.517	2.715	3.350	2.400	0.441	0.500	0.220	0.175
9	50	3	0.616	2.025	2.320	1.880	0.598	0.587	0.142	0.109
10	50	3	0.510	2.035	1.655	1.295	0.524	0.271	0.294	0.141

Abbreviations: F%, fibrosis ratio; IFTA, interstitial fibrosis and tubular atrophy score; MK, mean kurtosis; MD, mean diffusivity; Da, axial diffusivity; Dr, radial diffusivity; Ka, axial kurtosis; Kr, radial kurtosis; FA, fractional anisotropy; FAk, fractional anisotropy of kurtosis.

healthy volunteers.[42] Further studies involving a broader spectrum of kidney diseases may enhance the clinical value of Da, Dr, and other parameters as biomarkers for renal assessment.

Radial kurtosis (Kr), fractional anisotropy (FA), and kurtosis anisotropy (FAk) were all included in our analysis. However, they did not differ significantly across the three groups (Table 2), and only FAk was correlated significantly with renal pathology (Table 6). While FA is sensitive mainly to the integrity of tubular orientation arrangement,[43] the early damage in DN (such as glomerular sclerosis) has a weak effect on such integrity.[44] Because the renal cortex has a more disorganized microstructure than the medulla, imaging parameters that are sensitive to radial diffusion (like Kr) may be less effective at detecting disease-related changes. Cortical Kr values are high at baseline and show wide variability between individuals,[45] which can obscure subtle pathological effects. Although FAk was correlated significantly negatively with the fibrosis ratio and the IFTA score, it did not differ significantly across the three groups. In DKI, FAk has been proven to offer distinct and complementary microstructural contrast compared to FA, especially in areas with near orthogonal fiber arrangements and in deep brain structures.[46] The diagnostic performance of FAk was limited because FAk depends on ultra-high b-value imaging (≥2000 s/mm^2),[47] but cortical contrast at such b-values is often weak, and disease-related changes may be masked by inter-individual variability.

Existing investigations of MRI in kidney disease generally target patients whose CKD is caused by various factors, and the MRI parameters are mostly those frequently used in clinical practice (eg, ADC, D, etc). Some studies on CKD have reported that MK[48] and MD[44] have excellent diagnostic performance and clinical utility, and few studies reported on other DKI parameters (Da, Dr, Fak, etc). This work for the first time includes all DKI parameters, although it is

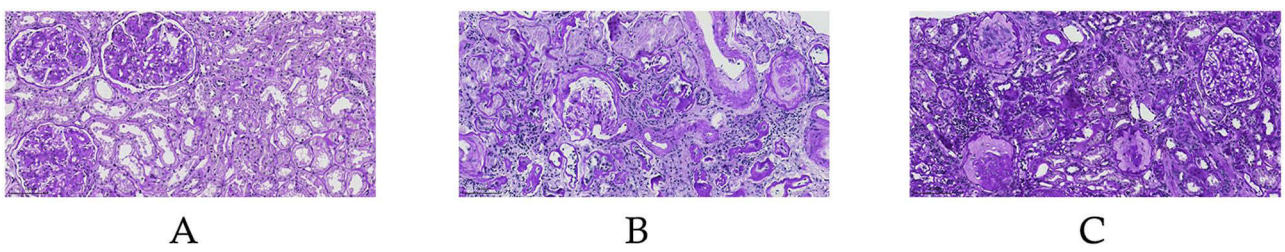

Figure 7 Pathological images (PAS staining) of renal biopsy. (**A**) Patient diagnosed with diabetes (Group DM). (**B**) Patient diagnosed with diabetic nephropathy and eGFR > 60 mL/min/1.73 m2 (Group Mild). (**C**) Patient diagnosed with diabetic nephropathy and eGFR ≤ 60 mL/min/1.73 m2 (Group Severe).

Table 6 Correlation Between Renal DKI Metrics and Pathology Parameters in DN Patients Who Received Renal Biopsy

DKI metrics (cortex)	F%		IFTA	
	r	*P*	*r*	*P*
MK	0.685	0.102	0.837	**0.039**
MD	−0.318	0.367	−0.509	0.144
Da	−0.202	0.575	−0.509	0.144
Dr	−0.551	0.105	−0.596	0.090
Ka	0.251	0.481	0.427	0.222
Kr	−0.012	0.978	0.210	0.561
FA	0.226	0.526	−0.110	0.787
FAk	−0.685	**0.034**	−0.809	**0.006**

Note: *P* values are typeset in boldface if they are less than 0.05.
Abbreviations: F%, percentage of fibrosis; IFTA, interstitial fibrosis and tubular atrophy; MK, mean kurtosis; MD, mean diffusivity; Da, axial diffusivity; Dr, radial diffusivity; Ka, axial kurtosis; Kr, radial kurtosis; FA, fractional anisotropy; FAk, fractional anisotropy of kurtosis.

Table 7 Diagnostic Value of DKI Metrics

	MK†	MD†	Da†	Dr†	Ka†
AUC†	0.922	0.865	0.787	0.774	0.910
95% CI†	0.843–1.000	0.756–0.973	0.640–0.934	0.629–0.919	0.824–0.996
Threshold	0.49	2.46	2.89	2.23	0.5
Sensitivity (%)	83.3	94.4	77.8	83.3	95.8
Specificity (%)	94.4	75	79.2	87.5	72.2
Youden index (Max)	0.777	0.694	0.57	0.557	0.68
p-value	<0.001	<0.001	<0.001	<0.001	<0.001

Notes: †The data describes the ability of the metrics to distinguish Group Severe from the other two groups combined (ie, Group Mild and Group DM).
Abbreviations: MK, mean kurtosis; MD, mean diffusivity; Da, axial diffusivity; Dr, radial diffusivity; Ka, axial kurtosis; AUC, area under the curve; CI, confidence interval.

limited to one type of CKD. Future studies can explore the utility of DKI in the diagnosis of other CKD, such as IgA nephropathy, membranous nephropathy, etc.

The limitations of this study are as follows. This is a single center study involving patients who visited our hospital. We included only 11 patients as the control (Group DM), and the number of patients was small for the other two groups too (Group Mild, 14; Group Severe, 29). Since we only had 10 biopsy samples, most DKI metrics were not significantly correlated ($P > 0.05$) with pathology parameters, and the connection between MK and conventional laboratory results (eg, eGFR, renal vascular lesions) was not thoroughly verified. We expect future studies with more biopsy samples to provide unequivocal conclusions. Moreover, this study is a cross-sectional study, and we did not have an external validation cohort. Future work that follows up the subjects identified by DKI will be essential. The diagnostic value also needs to be further compared between DKI and other models (eg, DTI-MRI, IVIM-MRI). Nevertheless, this study still demonstrated that DKI could serve to characterize the renal function and fibrosis of DN patients, and MK was an excellent non-invasive biomarker in this context.

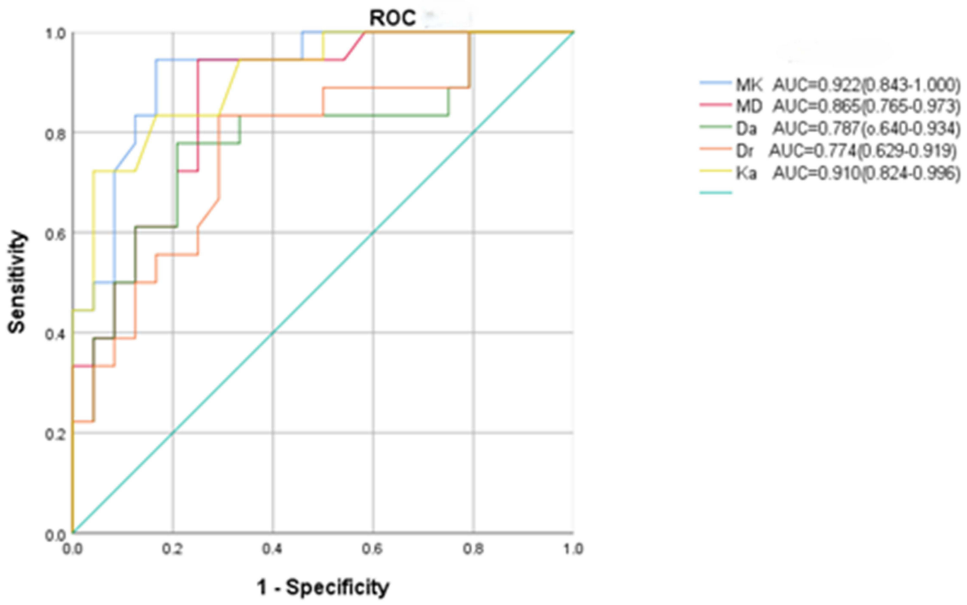

Figure 8 ROC curves of different DKI metrics in identifying patients with severe diabetic nephropathy.
Abbreviations: MK, mean kurtosis; MD, mean diffusivity; Da, axial diffusivity; Dr, radial diffusivity; Ka, axial kurtosis.

Conclusions

In summary, DKI is a powerful means for non-invasively evaluating the renal microstructure of DKD patients, surpassing traditional diffusion imaging techniques especially in capturing tissue complexity and heterogeneity. By differentiating renal cortical damage, it expedites the early detection of diabetic nephropathy and renal fibrosis. Among the DKI metrics, MK demonstrated the best diagnostic performance and is expected to become an important imaging biomarker for kidney disease, supporting not only accurate diagnosis and staging but also treatment efficacy evaluation and prognosis. The application of DKI is expected to widen as continuing research and technological advances (eg, the development of accelerated imaging sequences) tackle current challenges in scanning time, data processing, standardization, clinical validation, etc.

Abbreviations

DKI, Diffusion Kurtosis Imaging; DN, Diabetic nephropathy; DM, Diabetes mellitus; MK, Mean Kurtosis; MD, Mean Diffusivity; Da, Diffusivity Axial; Dr, Diffusivity Radial; Ka, Kurtosis Axial; Kr, Kurtosis Radial; FA, Fractional Anisotropy; Fak, Fractional Anisotropy of Kurtosis; ROC, Receiver Operating Characteristic; IFTA, Interstitial Fibrosis and Tubular Atrophy; eGFR, Estimated Glomerular Filtration Rate; Hb, Hemoglobin; CysC, Cystatin C; NGAL, Neutrophil Gelatinase-Associated Lipocalin; Scr, Serum Creatinine; ALB, Albumin; AUC, Area Under the Curve; ESRD, End-Stage Renal Disease; MRI, Magnetic Resonance Imaging; CT, Computed Tomography; DWI, Diffusion-Weighted Imaging; DTI, Diffusion Tensor Imaging; uACR, Urine Albumin-to-Creatinine Ratio; ARB, Angiotensin Receptor Blocker; ACEI, Angiotensin-Converting Enzyme Inhibitor; T1DM, Type 1 Diabetes Mellitus; HCT, Hematocrit; H&E, Hematoxylin and Eosin; PAS, Periodic Acid-Schiff; PASM, Periodic Acid-Silver Methenamine; ROIs, Regions of Interest; ICC, Intraclass Correlation Coefficient.

Ethics Approval and Consent to Participate

The Affiliated Hospital of Nantong University in China has reviewed and approved this research (approval No. 2019-K070). Written informed consent was obtained from all participants.

Acknowledgments

We are grateful to all patients who kindly agreed to participate in this study. We also thank the Affiliated Hospital of Nantong University for providing us with the research platform and for technical support.

Author Contributions

All authors made significant contributions to the study and participated in key aspects of the study, including conception, design, execution, data acquisition, data analysis, writing, and revision. All authors reviewed and approved the final manuscript and are jointly responsible for the research work and the content of the published article.

Funding

This study received funding from the following sources: National Key Research and Development Program of China (2023YFC3503501); Foundation of Jiangsu Province Research Hospital (YJXYY202204-XKB13); Postdoctoral Research Funding Scheme (BSH202412); and Nantong Technology Projects (MSZ2023112).

Disclosure

The authors declare no conflicts of interest in this work.

References

1. Lu Q, Zuo WZ, Ji XJ, et al. Ethanolic Ginkgo biloba leaf extract prevents renal fibrosis through Akt/mTOR signaling in diabetic nephropathy. *Phytomedicine*. 2015;22(12):1071–1078. doi:10.1016/j.phymed.2015.08.010
2. Hu Q, Chen Y, Deng X, et al. Diabetic nephropathy: focusing on pathological signals, clinical treatment, and dietary regulation. *Biomed Pharmacother*. 2023;159:114252. doi:10.1016/j.biopha.2023.114252
3. Natesan V, Kim SJ. Diabetic nephropathy - a review of risk factors, progression, mechanism, and dietary management. *Biomol Ther*. 2021;29(4):365–372. doi:10.4062/biomolther.2020.204
4. Selby NM, Taal MW. An updated overview of diabetic nephropathy: diagnosis, prognosis, treatment goals and latest guidelines. *Diabetes Obes Metab*. 2020;22 Suppl 1:3–15. doi:10.1111/dom.14007
5. Zheng X, Gao Y, Huang Y, et al. Clinical value of noninvasive lens advanced glycation end product detection in early screening and severity evaluation of patients with diabetic kidney disease. *BMC Nephrol*. 2023;24(1):379. doi:10.1186/s12882-023-03428-3
6. Sansone F, Tonacci A. Non-invasive diagnostic approaches for kidney disease: the role of electronic nose systems. *Sensors*. 2024;24(19):6475. doi:10.3390/s24196475
7. Shaw CB, Jensen JH. Recent computational advances in denoising for magnetic resonance diffusional kurtosis imaging (DKI). *J Indian Inst Sci*. 2017;97(3):377–390. doi:10.1007/s41745-017-0036-2
8. Zhuo J, Gullapalli RP. Diffusion Kurtosis Imaging. In: Mannil M, Winklhofer SFX, editors. *Neuroimaging Techniques in Clinical Practice: Physical Concepts and Clinical Applications*. Cham, Switzerland: Springer Nature Switzerland AG; 2020:215–228.
9. Giannelli M, Toschi N. On the use of trace-weighted images in body diffusional kurtosis imaging. *Magn Reson Imaging*. 2016;34(4):502–507. doi:10.1016/j.mri.2015.12.013
10. Arab A, Wojna-Pelczar A, Khairnar A, Szabó N, Ruda-Kucerova J. Principles of diffusion kurtosis imaging and its role in early diagnosis of neurodegenerative disorders. *Brain Res Bull*. 2018;139:91–98. doi:10.1016/j.brainresbull.2018.01.015
11. Andica C, Kamagata K, Hatano T, et al. MR biomarkers of degenerative brain disorders derived from diffusion imaging. *J Magn Reson Imaging*. 2020;52(6):1620–1636. doi:10.1002/jmri.27019
12. Karlsen RH, Einarsen C, Moe HK, et al. Diffusion kurtosis imaging in mild traumatic brain injury and postconcussional syndrome. *J Neurosci Res*. 2019;97(5):568–581. doi:10.1002/jnr.24383
13. Hui ES, Fieremans E, Jensen JH, et al. Stroke assessment with diffusional kurtosis imaging. *Stroke*. 2012;43(11):2968–2973. doi:10.1161/STROKEAHA.112.657742
14. Ota M, Noda T, Sato N, et al. The use of diffusional kurtosis imaging and neurite orientation dispersion and density imaging of the brain in major depressive disorder. *J Psychiatr Res*. 2018;98:22–29. doi:10.1016/j.jpsychires.2017.12.011
15. Goghari VM, Kusi M, Shakeel MK, et al. Diffusion kurtosis imaging of white matter in bipolar disorder. *Psychiatry Res Neuroimaging*. 2021;317:111341. doi:10.1016/j.pscychresns.2021.111341
16. Huang Y, Chen X, Zhang Z, et al. MRI quantification of non-Gaussian water diffusion in normal human kidney: a diffusional kurtosis imaging study. *NMR Biomed*. 2015;28(2):154–161. doi:10.1002/nbm.3235
17. Pentang G, Lanzman RS, Heusch P, et al. Diffusion kurtosis imaging of the human kidney: a feasibility study. *Magn Reson Imaging*. 2014;32(5):413–420. doi:10.1016/j.mri.2014.01.006
18. Zhou H, Zhang J, Zhang XM, et al. Noninvasive evaluation of early diabetic nephropathy using diffusion kurtosis imaging: an experimental study. *Eur Radiol*. 2021;31(4):2281–2288. doi:10.1007/s00330-020-07322-6
19. Zhang D, Geng X, Suo S, Zhuang Z, Gu Y, Hua J. The predictive value of DKI in breast cancer: does tumour subtype affect pathological response evaluations? *Magn Reson Imaging*. 2022;85:28–34. doi:10.1016/j.mri.2021.10.013
20. Pang H, Dang X, Ren Y, et al. DKI can distinguish high-grade gliomas from IDH1-mutant low-grade gliomas and correlate with their different nuclear-to-cytoplasm ratio: a localized biopsy-based study. *Eur Radiol*. 2024;34(11):7539–7551. doi:10.1007/s00330-023-10325-8
21. Cheng Q, Ren A, Xu X, et al. Application of DKI and IVIM imaging in evaluating histologic grades and clinical stages of clear cell renal cell carcinoma. *Front Oncol*. 2023;13:1203922. doi:10.3389/fonc.2023.1203922
22. Liu Y, Zhang GM, Peng X, Li X, Sun H, Chen L. Diffusion kurtosis imaging as an imaging biomarker for predicting prognosis in chronic kidney disease patients. *Nephrol Dial Transplant*. 2022;37(8):1451–1460. doi:10.1093/ndt/gfab229
23. Aziz S, Harun SN, Ghadzi SMS. Disease progression modeling of estimated glomerular filtration rate (eGFR): a pharmacometrics approach. *J Diabetes*. 2025;176:e70104. doi:10.1111/1753-0407.70104

24. Levey AS, Stevens LA, Schmid CH, et al. A new equation to estimate glomerular filtration rate. *Annal Intern Med*. 2009;150(9):604–612. doi:10.7326/0003-4819-150-9-200905050-00006
25. Zhu X, Xiong X, Yuan S, et al. Validation of the interstitial fibrosis and tubular atrophy on the new pathological classification in patients with diabetic nephropathy: a single-center study in China. *J Diabetes Complications*. 2016;30(3):537–541. doi:10.1016/j.jdiacomp.2015.12.002
26. Jensen JH, Helpern JA. MRI quantification of non-Gaussian water diffusion by kurtosis analysis. *NMR Biomed*. 2010;23(7):698–710. doi:10.1002/nbm.1518
27. Rosenkrantz AB, Padhani AR, Chenevert TL, et al. Body diffusion kurtosis imaging: basic principles, applications, and considerations for clinical practice. *J Magn Reson Imaging*. 2015;42(5):1190–1202. doi:10.1002/jmri.24985
28. Paydar A, Fieremans E, Nwankwo JI, et al. Diffusional kurtosis imaging of the developing brain. *AJNR Am J Neuroradiol*. 2014;35(4):808–814. doi:10.3174/ajnr.A3764
29. Serulle Y, Pawar RV, Eubig J, et al. Diffusional kurtosis imaging in hydrocephalus. *Magn Reson Imaging*. 2015;33(5):531–536. doi:10.1016/j.mri.2015.02.009
30. Marrale M, Collura G, Brai M, et al. Physics, techniques and review of neuroradiological applications of diffusion kurtosis imaging (DKI). *Clin Neuroradiol*. 2016;26(4):391–403. doi:10.1007/s00062-015-0469-9
31. E TN-S, Udby blicher J, Møller Thastum M, et al. Microstructural changes in the brain after long-term post-concussion symptoms: a randomized trial. *J Neurosci Res*. 2021;99(3):872–886. doi:10.1002/jnr.24773
32. Steven AJ, Zhuo J, Melhem ER. Diffusion kurtosis imaging: an emerging technique for evaluating the microstructural environment of the brain. *AJR Am J Roentgenol*. 2014;202(1):W26–33. doi:10.2214/AJR.13.11365
33. Hu W, Qiu Z, Huang Q, et al. Microstructural changes of the white matter in systemic lupus erythematosus patients without neuropsychiatric symptoms: a multi-shell diffusion imaging study. *Arthritis Res Ther*. 2024;26(1):110. doi:10.1186/s13075-024-03344-3
34. Henriques RN, Henson R, Cam CAN, Correia MM. Unique information from common diffusion MRI models about white-matter differences across the human adult lifespan. *Imaging Neurosci*. 2023;1:1–25.
35. Yao W, Zheng J, Han C, et al. Integration of quantitative diffusion kurtosis imaging and prostate specific antigen in differential diagnostic of prostate cancer. *Medicine*. 2021;100(35):e27144. doi:10.1097/MD.0000000000027144
36. Pruijm M, Milani B, Pivin E, et al. Reduced cortical oxygenation predicts a progressive decline of renal function in patients with chronic kidney disease. *Kidney Int*. 2018;93(4):932–940. doi:10.1016/j.kint.2017.10.020
37. Bonventre JV, Yang L. Cellular pathophysiology of ischemic acute kidney injury. *J Clin Invest*. 2011;121(11):4210–4221. doi:10.1172/JCI45161
38. Gholampour F, Masjedi F, Janfeshan S, Karimi Z. Remote limb ischemic pre-conditioning prevents renal Ischemia/reperfusion injury in rats by modulating oxidative stress and TNF-α/NF-κB/TGF-/βapelin signaling pathway. *Mol Biol Rep*. 2024;52(1):4. doi:10.1007/s11033-024-10109-3
39. Li C, Yu Y, Zhu S, et al. The emerging role of regulated cell death in ischemia and reperfusion-induced acute kidney injury: current evidence and future perspectives. *Cell Death Discov*. 2024;10(1):216. doi:10.1038/s41420-024-01979-4
40. Hueper K, Hartung D, Gutberlet M, et al. Magnetic resonance diffusion tensor imaging for evaluation of histopathological changes in a rat model of diabetic nephropathy. *Invest Radiol*. 2012;47(7):430–437. doi:10.1097/RLI.0b013e31824f272d
41. Liang P, Li S, Yuan G, et al. Noninvasive assessment of clinical and pathological characteristics of patients with IgA nephropathy by diffusion kurtosis imaging. *Insights Imaging*. 2022;13(1):18. doi:10.1186/s13244-022-01158-y
42. Wen D, Xu C, Deng L, et al. Monoexponential, biexponential, stretched-exponential and kurtosis models of diffusion-weighted imaging in kidney assessment: comparison between patients with primary aldosteronism and healthy controls. *Abdom Radiol*. 2023;484:1340–1349. doi:10.1007/s00261-023-03833-0
43. Yu W, Yan W, Yi J, et al. Application of diffusion kurtosis imaging and blood oxygen level-dependent magnetic resonance imaging in kidney injury associated with ANCA-associated vasculitis. *Tomography*. 2024;107:970–982. doi:10.3390/tomography10070073
44. Yang D, Tian C, Liu J, et al. Diffusion tensor and kurtosis MRI-based radiomics analysis of kidney injury in type 2 diabetes. *J Magn Reson Imaging*. 2024;605:2078–2087.
45. Wang B, Wang Y, Li L, et al. Diffusion kurtosis imaging and arterial spin labeling for the noninvasive evaluation of persistent post-contrast acute kidney injury. *Magn Reson Imaging*. 2022;87:47–55. doi:10.1016/j.mri.2021.12.004
46. He X, Zhao X, Sun Y, Geng P, Zhang X. Application of TBSS-based machine learning 468 models in the diagnosis of pediatric autism. *Front Neurol*. 2022;13:1078147. doi:10.3389/fneur.2022.1078147
47. Li A, Yuan G, Hu Y, et al. Renal functional and interstitial fibrotic assessment with non-Gaussian diffusion kurtosis imaging. *Insights Imaging*. 2022;131:70. doi:10.1186/s13244-022-01215-6
48. Yuan G, Liao Z, Liang P, et al. Noninvasive grading of renal interstitial fibrosis and prediction of annual renal function loss in chronic kidney disease: the optimal solution of seven MR diffusion models. *Ren Fail*. 2025;471:2480751. doi:10.1080/0886022X.2025.2480751